The tumour-associated antigen L6 (L6-Ag) is recruited to the tetraspanin-enriched microdomains: implication for tumour cell motility

Tamara Lekishvili, Elisa Fromm, Michelle Mujoomdar and Fedor Berditchevski*

Cancer Research UK Institute for Cancer Studies, The University of Birmingham, Edgbaston, Birmingham, B15 2TT, UK

*Author for correspondence (e-mail: f.berditchevski@bham.ac.uk)

Accepted 21 November 2007
J. Cell Sci. 121, 685-694 Published by The Company of Biologists 2008
doi:10.1242/jcs.020347

Summary

Tumour-associated antigen L6 (L6-Ag, also known as TM4SF1) regulates tumour cell motility and invasiveness. We found that L6-Ag is abundant on the plasma membrane and on intracellular vesicles, on which it is co-localised with the markers for late endosomal/lysosomal compartments, including Lamp1/Lamp2 proteins and LBPA. Antibody internalisation and live-imaging experiments suggested that L6-Ag is targeted to late endocytic organelles (LEO) predominantly via a biosynthetic pathway. Mapping experiments showed that the presence of transmembrane regions is sufficient for directing L6-Ag to LEO. On the plasma membrane, L6-Ag is associated with tetraspanin-enriched microdomains (TERM). All three predicted cytoplasmic regions of L6-Ag are crucial for the effective recruitment of the protein to TERM. Recruitment to TERM correlated with the pro-migratory activity of L6-Ag. Depletion of L6-Ag with siRNA has a selective effect on the surface expression of tetraspanins CD63 and CD82. By contrast, the expression levels of other tetraspanins and β1 integrins was not affected. We found that L6-Ag is ubiquitylated and that ubiquitylation is essential for its function in cell migration. These data suggest that L6-Ag influences cell motility via TERM by regulating the surface presentation and endocytosis of some of their components.

Key words: L6 antigen, Tetraspan, Late endosomes, Migration, Tetraspanin

Introduction

A small (~21 kD, 202 amino acids) four-transmembrane-domain protein L6 (L6-Ag, also known as TM4SF1) had been originally described as a tumour-specific antigen for various human epithelial malignancies (Hellström et al., 1986; Marken et al., 1992). Initially, L6-Ag was classified as a member of the tetraspanin superfamily of membrane proteins (Marken et al., 1992; Wright and Tomlinson, 1994). However, it was later recognised that L6-Ag belongs to a distinct family of the four-transmembrane-domain proteins (Wright et al., 2000), which also includes L6H (TM4SF5) (Muller-Pillasch et al., 1998), L6D (Wright et al., 2000) and il-TMP (Wice and Gordon, 1995). Transcripts of L6-Ag were detected in various normal mouse tissues: most prominently in endothelium, lung and skin (Edwards et al., 1995). A search for the L6-Ag transcripts in the human expressed sequence tags (EST) database revealed that the *L6-Ag* gene is also transcribed in a variety of normal human tissues (our unpublished results).

Recent studies indicate that L6-Ag is involved in the migration of immortalised keratinocytes in vitro and potentiates invasiveness (and metastasis) of lung cancer cells in an animal model (Kao et al., 2003; Storim et al., 2001). It has been recently shown that L6-Ag is associated with CD13 (aminopeptidase N) and this interaction might be important in the pro-invasive activity of the protein (Chang et al., 2005). In addition, the C-terminal cytoplasmic portion of L6-Ag contains an unconventional PDZ-domain-binding motif (X-Tyr-X-Cys), which binds to syntenin-2 (SITAC), a PDZ-domain-containing protein (Borrell-Pages et al., 2000). Interestingly, syntenin-2 can, in turn, interact with syntenin-1, a closely related protein (Koroll et al., 2001). This interaction might prove crucial for the biological function of L6-Ag because, potentially, syntenin-1 could bridge the L6-Ag–syntenin-2 complex with its transmembrane and cytoplasmic partners (e.g. syndecans, Eph receptors, merlin) (Sarkar et al., 2004).

The dynamics of transmembrane adhesion receptors on the plasma membrane play an important role in cell motility (Jones et al., 2006). Indeed, interference with endocytosis and recycling of various integrin heterodimers has a negative effect on persistent and random cell migration (White et al., 2007). Various cytoplasmic and transmembrane proteins have been implicated in integrin trafficking, including various Rab proteins, protein kinase D1 (PKCmu) (Roberts et al., 2001), ACAP1 (CENTB1) (Li et al., 2005), PKCε (Ivaska et al., 2002) and tetraspanins (Winterwood et al., 2006). In addition, recruitment of integrins to specific microdomains on the plasma membrane controls their endo-exocytic cycle during migration (Fabbri et al., 2005).

Four-transmembrane-domain proteins of the tetraspanin superfamily are principal structural components of tetraspanin-enriched microdomains, TERM (also known as a tetraspanin web). Through a complex network of protein-protein and protein-lipid interactions, tetraspanins recruit various transmembrane and cytoplasmic proteins into TERM, including integrins, receptors tyrosine kinases, protein and lipid kinases, and PDZ-domain-containing proteins. The role of TERM in cell motility is supported by numerous reports describing how changes in the expression levels of various tetraspanins can either facilitate or suppress cell migration (Berditchevski, 2001; Hemler, 2005). More-detailed biochemical analyses showed that tetraspanins regulate various integrin-mediated signalling pathways that are crucial for cell motility, including

activation of PI3-kinase, Erk1/2 and Cdc42 (Sawada et al., 2003; Shigeta et al., 2003; Sugiura and Berditchevski, 1999; Takeda et al., 2007). In addition, recent evidence shows that tetraspanins regulate surface expression and endocytosis of their transmembrane partners, including integrins (He et al., 2005; Shoham et al., 2003; Winterwood et al., 2006).

Trafficking of transmembrane proteins to the plasma membrane and various intracellular organelles is controlled at multiple levels and involves recognition of particular targeting signals by specific adapter complexes (Bonifacino and Traub, 2003). In many single-pass transmembrane proteins, these signals represent a linear sequence in the cytoplasmic portion of the protein. These include a classical tyrosine-based recognition sequence (Yxxϕ) and various di-leucine-based motifs (Bonifacino and Traub, 2003). By contrast, targeting of polytopic transmembrane cargos might require spatial coordination of sequences from the different parts of the protein (Leube, 1995).

In order to understand how L6-Ag might contribute to the migratory process, we analysed cellular distribution of the protein. Our results show that L6-Ag is abundant on the cell surface and on late endocytic organelles. On the cell surface, L6-Ag is recruited to TERM and the pro-migratory activity of the protein correlates with its ability to associate with tetraspanins. Downregulation of L6-Ag with specific siRNAs resulted in a specific increase in the surface levels of tetraspanins CD63 and CD82. Taken together, our data suggest that L6-Ag regulates cell motility via tetraspanin-enriched microdomains.

Results

L6-Ag is abundant on the plasma membrane and intracellular vesicles

It has been previously shown that L6-Ag potentiates migration and invasion of lung carcinoma cells (Chang et al., 2005; Kao et al., 2003). Similarly, we found that ectopic expression of the protein in breast cancer cells (MCF-7) enhances their migration towards fibronectin (Fig. 1A). Conversely, downregulation of L6-Ag expression with specific siRNAs in MDA-MB-231 and BT-549, two highly motile breast carcinoma cell lines, resulted in suppression of their motility (Fig. 1B,C). A previous study suggested that L6-Ag regulates cell motility through its interaction with aminopeptidase N (CD13) (Chang et al., 2005). However, we found that both MCF-7 and MDA-MB-231 cells express negligible levels of this protein (results are not shown), thereby suggesting that CD13 is not required for L6-Ag to manifest its pro-migratory activity. As a first step towards understanding how L6-Ag might affect migration of breast cancer cells, we examined the subcellular localisation of the protein. Flow cytometry analysis and immunofluorescence staining showed that L6-Ag is abundant on the plasma membrane and on the intracellular organelles of MDA-MB-231 cells (results not shown). The immunoprecipitation experiments showed that, in BT549 cells, ~20-25% of the protein is localised on the cell surface (results are not shown). The plasma membrane pool of L6-Ag was very labile and was almost completely lost even after brief permeabilisation with Triton X-100. To establish the identity of the L6-Ag-positive organelles, cells were simultaneously stained with monoclonal antibodies (mAbs) against L6-Ag and against various compartmental markers. As illustrated in Fig. 2, L6-Ag antigen was partially co-localised with Lamp1 and LBPA, well-established markers for late endosomal and lysosomal compartments. By contrast, no significant L6-Ag staining was detected in the Golgi or on early endosomes (EEA1-positive vesicles) (Fig. 2). Similarly, when ectopically expressed in L6-Ag-negative MCF-7 cells, the protein was found in Lamp2-positive vesicles but was excluded from EEA1-positive early endosomes (results not shown). Hereafter, we refer to L6-Ag-positive organelles as late endocytic organelles (LEO).

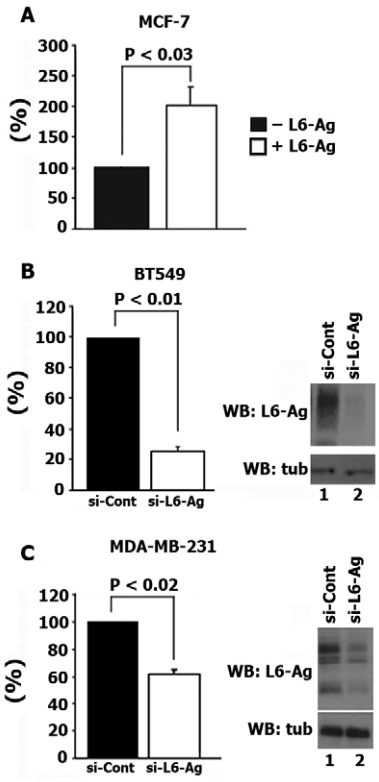

Fig. 1. L6-Ag regulates motility of breast cancer cells. (A) MCF-7 cells were co-transfected with plasmids encoding L6-Ag and GFP. Migration experiments towards fibronectin were performed 48 hours after transfection. (B,C) Cells were electroporated with control siRNA (si-Cont) or siRNA that targets L6-Ag (si-L6-Ag). Migration experiments were performed 72 hours after transfection. Migration was quantified by counting cells in seven random fields per membrane (~10-30 cells/field) as described in detail in Materials and Methods. Data are reported as fold increases/decreases over migration of cells transfected with either control plasmid (GFP, A) or control siRNA (B,C). Data (all graph panels) are shown as mean ± standard deviation (s.d.) calculated from at least three separate experiments each performed in triplicate. *P* values were calculated using the two-tailed *t*-test. Right panels show representative western blots (WB) using lysates prepared 72 hours after transfection.

L6-Ag is ubiquitylated

Ubiquitylation is not required for targeting of L6-Ag to late endocytic organelles

We wished to establish whether enrichment of L6-Ag on LEO is linked to the pro-migratory activity of the protein. As a first step towards this goal, we wanted to identify a region(s) responsible for targeting L6-Ag to LEO. The primary structure of L6-Ag does not reveal apparent sorting motif(s)/sequence(s) that would explain its localisation to LEO. It has been previously reported that ubiquitylation plays an important role in the sorting of transmembrane proteins to late endosomes (Raiborg et al., 2003). Hence, we investigated whether L6-Ag is ubiquitylated and, if it is, the contribution of ubiquitylation in the targeting of L6-Ag to LEO. As shown in Fig. 3A, two ubiquitylated species of the

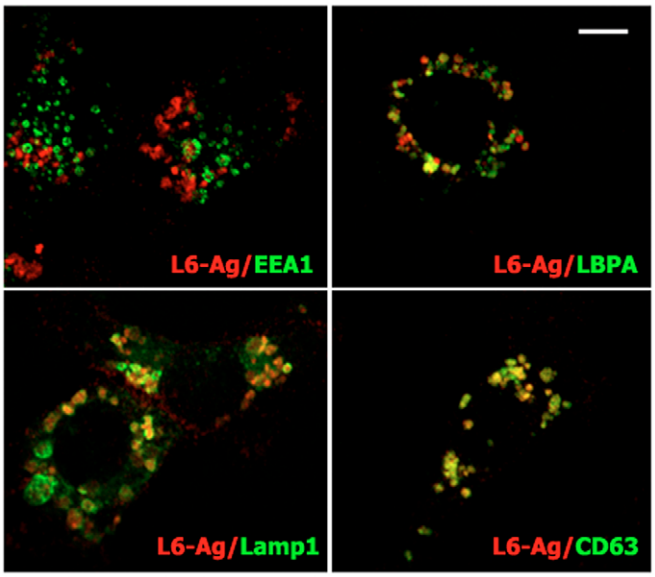

Fig. 2. L6-Ag is found in late endocytic organelles. MDA-MB-231 cells were grown on glass coverslips, fixed with 2% paraformaldehyde and permeabilised with 0.1% Triton X-100. Immunofluorescence staining was carried out using mouse mAb to human L6-Ag (IgG2a) in combination with mouse mAbs to proteins localised to various intracellular compartments (all IgG1): EEA1, early endosomes; LBPA, late endosomes; Lamp1, late endosomes/lysosomes. Staining was visualised using Alexa-Fluor-594-conjugated goat anti-mouse IgG2a Ab (red) and Alexa-Fluor-488-conjugated goat anti-mouse IgG1 Ab (green). Shown are representative images acquired using a LSM510 microscope. Note that, after permeabilisation, surface pools of L6-Ag and CD63 are almost completely lost. Scale bar: 10 μm.

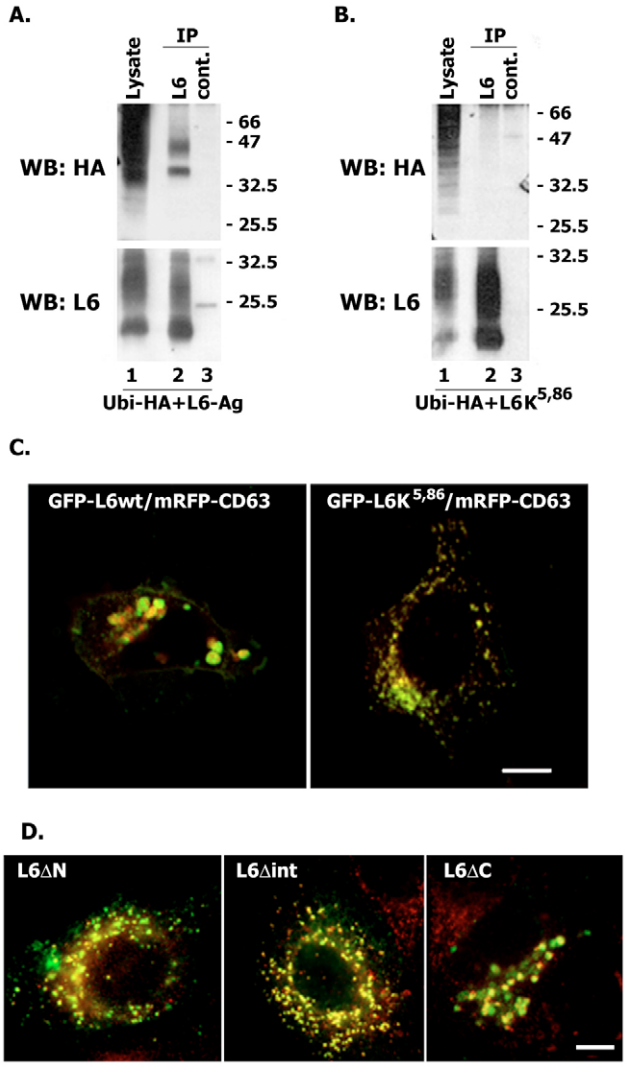

Fig. 3. L6-Ag is ubiquitylated. Cellular distribution of ubiquitylation-deficient L6-Ag. (A,B) 293T cells were transiently transfected with the plasmids encoding wild-type L6-Ag (A) or L6K^{5,86} (B) and HA-tagged ubiquitin. 48 hours later, cells were lysed in 1% Triton X-100 and the immunoprecipitation (IP) was carried out using the anti-L6-Ag mAb (lanes 2) or a negative control mAb (lanes 3). The protein lysates were used as a positive control for transfection (lanes 1). Proteins were resolved in 11% SDS-PAGE and transferred to nitrocellulose membranes. The membranes were probed with either anti-HA polyclonal Ab or the anti-L6-Ag mAb (L6pke). (C) MCF-7 cells were co-transfected with the plasmid encoding GFP-L6-Ag [wild type (wt), or GFP-L6K^{5,86}] and mRFP-CD63. Co-distribution of tagged proteins was analysed 48 hours after transfection. Shown are representative images acquired using a LSM510 microscope. (D) MCF-7 cells were transfected with the plasmid encoding L6-Ag mutants and 48 hours later the cells were processed for double-immunofluorescence staining using specific Abs as described in the legend to Fig. 2. Staining was visualised using Alexa-Fluor-488-conjugated goat anti-mouse IgG2a Ab (green, L6-Ag) and Alexa-Fluor-594-conjugated goat anti-mouse IgG1 Ab (red). Shown is the co-distribution of L6-Ag mutants and Lamp2. Scale bars: 10 μm.

protein can be immunoprecipitated with the anti-L6-Ag mAb. In the control experiments we found that tetraspanin proteins CD151 and CD63 did not incorporate ubiquitin under the same experimental conditions (results not shown). Predicted cytoplasmic regions of L6-Ag contain two lysines (Lys^{5} in the N-terminal cytoplasmic part and Lys^{86} in the cytoplasmic region between the predicted second and third transmembrane domains) that can potentially serve as acceptor sites for the ubiquitin moiety. Indeed, mutation of these residues to threonines completely abolished ubiquitylation of L6-Ag (Fig. 3B). We then examined the role of ubiquitylation in the subcellular distribution of L6-Ag. The overall distribution of a GFP-tagged ubiquitylation-deficient mutant (GFP-L6K^{5,86}) was similar to that of the wild-type protein: both proteins were found in small puncta scattered throughout the cytoplasm (Fig. 3C). Occasionally, we detected the GFP-tagged proteins in enlarged organelles. These organelles were found predominantly in the perinuclear area of the cells. The size of the L6-Ag-positive organelles varied from cell to cell, reaching up to ~1.5 μm in diameter. More-detailed analysis showed that the enlarged organelles were observed more frequently in cells expressing the wild-type protein: ~20-25% versus 10-15% in cells expressing GFP-L6K^{5,86}. Nonetheless, both small puncta and enlarged organelles were positive for CD63, thereby suggesting that ubiquitylation is not required for targeting of L6-Ag to LEO.

We then considered a possible contribution of predicted cytoplasmic regions: the N-terminus (amino acids 1-7), the intracellular loop (amino acids 72-92) and the C-terminus (amino acids 185-202). These regions of the protein were substituted for the HA-tag sequence (YPYDVPDYA) to generate L6ΔN, L6Δint and L6ΔC mutants. As shown in Fig. 3D, all three mutants were efficiently targeted to Lamp2-positive organelles when expressed in MCF-7 cells. Taken together, these data indicate that targeting of L6-Ag to LEO is independent of cytoplasmic regions of the protein.

The contribution of transmembrane domains to targeting of L6-Ag to LEO

To assess the contribution of transmembrane regions, we generated a set of constructs encoding L6-Ag–L6H chimeric proteins (Fig. 4A). Although L6H is closely related to L6-Ag (~50% of overall identity) and can be ubiquitylated (data not shown), it is localised to intracellular organelles that are negative for Lamp2 (Fig. 4B). We found that separate substitutions of the cytoplasmic or extracellular regions of L6-Ag for corresponding sequences of L6H does not prevent localisation of the chimeric proteins to Lamp2-positive organelles (Fig. 4B). Hence, the presence of transmembrane regions is sufficient to direct L6-Ag to LEO.

Analysis of trafficking of L6-Ag in MCF-7 cells

To analyse whether there exists a dynamic exchange between the LEO and plasma membrane pools of L6-Ag, we performed short-term live recordings (up to 15 minutes) of cells expressing GFP-L6. We found that L6-Ag-positive large perinuclear organelles were almost completely immobile (Fig. 5A). Occasionally, we observed that centrally located smaller organelles moved towards and fused with the cluster of larger L6-Ag-positive organelles (Fig. 5B). In some cells, we detected separation of small puncta from the plasma membrane. Although these peripherally located L6-Ag-positive vesicles were highly dynamic, no persistent directional movement of these vesicles towards the perinuclear cluster was observed. We also used the Ab-internalisation assay to examine whether L6-Ag can be routed to LEO from the cell surface. Cell labelling was carried out at 4°C and internalisation was subsequently induced after temperature of the media was shifted to 37°C. Surprisingly, even after 7 hours of incubation at 37°C, we were unable to detect the anti-L6-Ag mAb in Lamp2-positive organelles (Fig. 6A). By contrast, we observed that, within first 4 hours after the temperature shift, the anti-CD63 mAbs were internalised and detected in the L6-Ag-positive structures (Fig. 6B). These data suggest that there was no constitutive targeting of L6-Ag from the surface to LEO under normal growth conditions. Although these results do not completely rule out a possibility that a certain proportion of L6-Ag might be delivered to LEO via the endocytic route, they strongly suggest that the majority of the protein is targeted to late endocytic compartments directly from the trans-Golgi network (TGN).

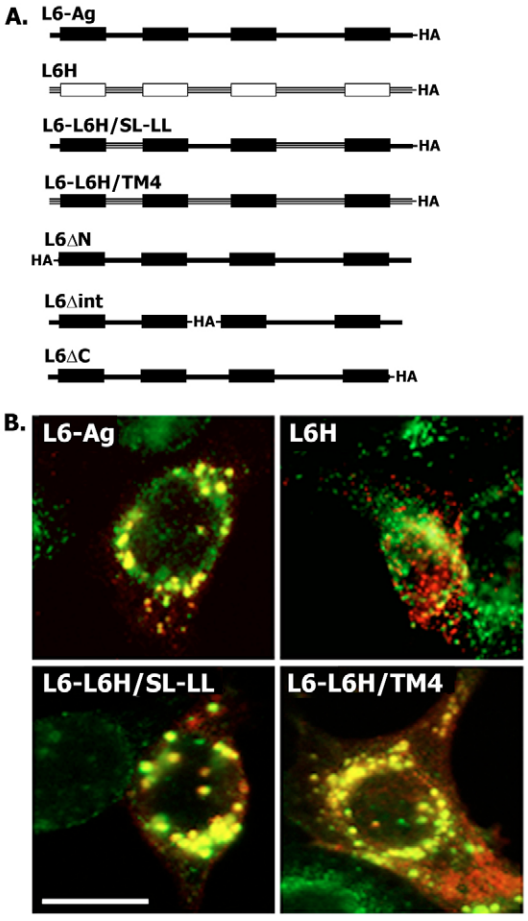

Fig. 4. The presence of transmembrane domains is sufficient to direct trafficking of L6 to late endocytic organelles. (A) Schematic diagram shows the constructs used for transfection of MCF-7 cells. (B) MCF-7 cells were transfected with the plasmid encoding the L6H-HA, L6-Ag-HA and L6-L6H chimeras, and 48 hours later the cells were processed for double-immunofluorescence staining using specific Abs as described in the legend to Fig. 2. Co-distribution of the tagged proteins with Lamp2 was analysed using anti-HA mAb F7 (IgG2a) and anti-Lamp2 mAb H4B4 (IgG1). Staining was visualised using Alexa-Fluor-594-conjugated goat anti-mouse IgG2a Ab (red) and Alexa-Fluor-488-conjugated goat anti-mouse IgG1 (green). Scale bar: 20 μm.

L6-Ag is associated with tetraspanin-enriched microdomains

The data presented above suggest that the pro-migratory activity of L6-Ag does not rely on the dynamic exchange between LEO- and surface pools of the protein. This led us to focus on the pool of L6-Ag associated with the plasma membrane. Specifically, using cell biotinylation, we wished to identify surface-associated partners for L6-Ag. Initial immunoprecipitation experiments showed that L6-Ag itself cannot be labelled with biotin using a standard surface-biotinylation protocol. However, L6-Ag could be co-immunoprecipitated with a number of biotin-labelled cell surface proteins (Fig. 7A, lane 1). Notably, a similar pattern of immunoprecipitated proteins was observed when we used the mAb

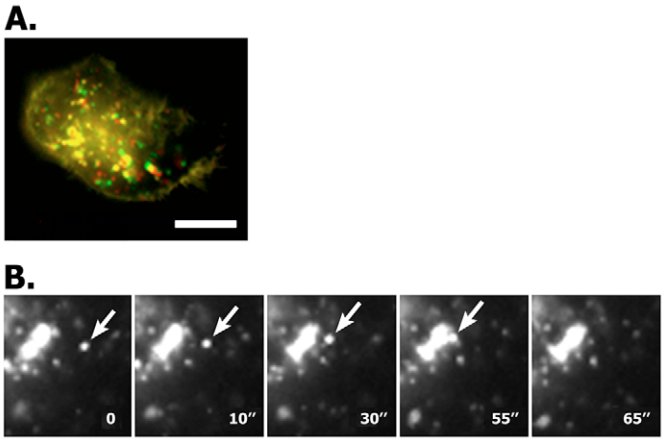

Fig. 5. Motility of L6-Ag-positive vesicles. MCF-7 cells were transiently transfected with the plasmid encoding GFP–L6-Ag and 48 hours later motility of the L6-Ag-positive endosomes was analysed by time-lapse video microscopy. Images were collected every 3 seconds for 1 minute (A) or every 3-5 seconds for 2 minutes (B). (A) Represents a superposition of the first and the last images artificially coloured in red and green, respectively. (B) Arrows point to a vesicle that fused with the enlarged L6-Ag-positive endosomes (video sequence). Scale bar: 10 μm.

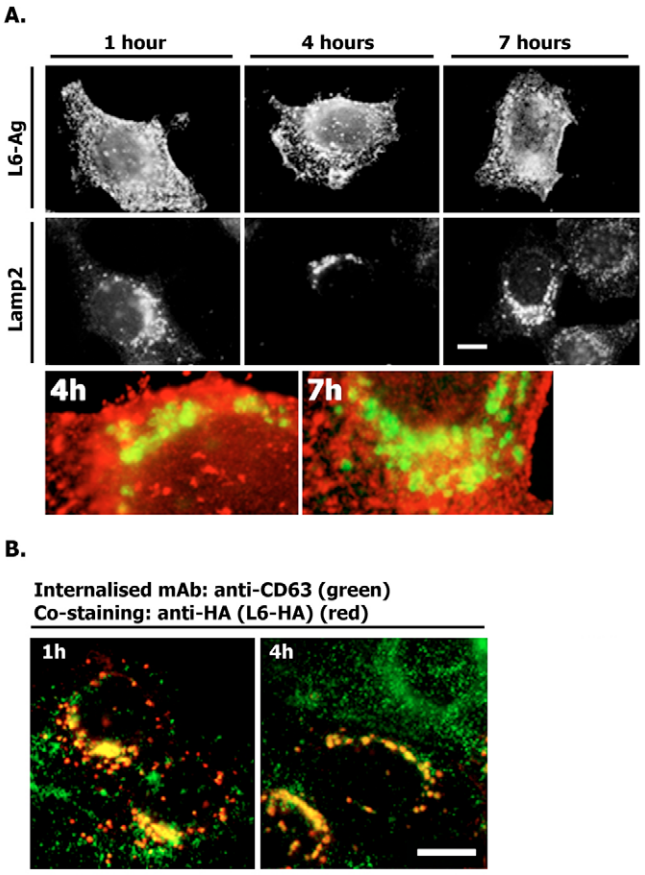

Fig. 6. Internalisation of surface-labelled L6-Ag and CD63. (A) MCF-7 cells were transiently transfected with the plasmid encoding HA–L6-Ag. 48 hours later, cells were surface labelled with the anti-L6-Ag mAb (L6, IgG2a) for 1 hour at 4°C and then placed to 37°C for the indicated durations. Cells were subsequently fixed and permeabilised as described in the legend to Fig. 2. The internalised mAbs were visualised with Alexa-Fluor-594-conjugated goat anti-mouse IgG2a (red). Late endocytic organelles were visualised with anti-Lamp2 mAb and Alexa-Fluor-488-conjugated goat anti-mouse IgG1 Ab (green). (B) MCF-7 cells were prepared for the experiments as described in A except that they were incubated with the anti-CD63 mAb (6H1, IgG1) instead of the anti-L6-Ag mAb. The internalised mAbs were visualised with Alexa-Fluor-488-conjugated goat anti-mouse IgG1 Ab (green). Late endocytic organelles were visualised with the anti-HA mAb (F7, IgG2a) and Alexa-Fluor-594-conjugated goat anti-mouse IgG2a Ab (red). Scale bars: 10 μm.

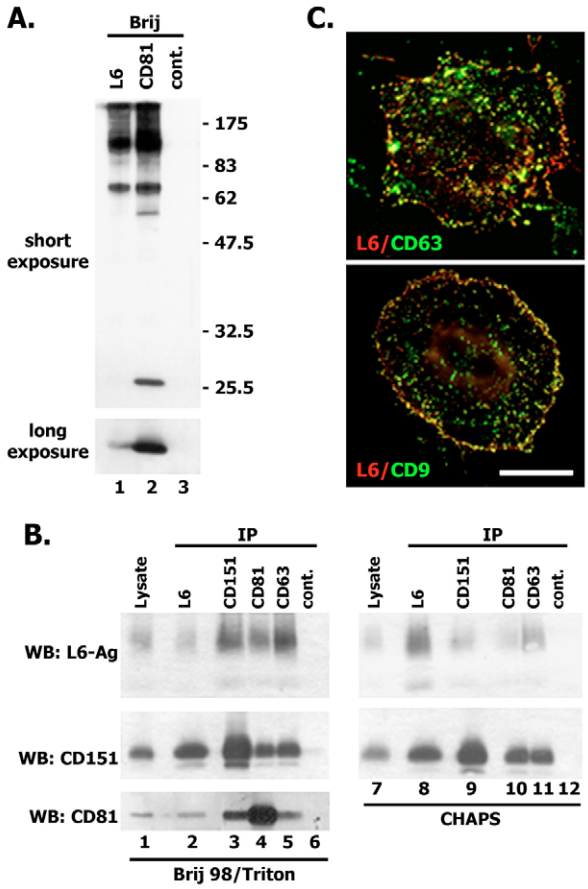

Fig. 7. L6-Ag is associated with tetraspanins. (A) HT1080 cells were surface labelled with EZ-link Sulfo-NHS-LC-biotin and lysed in 0.8% Brij98/0.2% Triton X-100. Protein complexes were immunoprecipitated with anti-L6-Ag mAb (lane 1), anti-CD81 and mAb M38 (lane 2) or control mAb (lane 3). Immunocomplexes were separated in 11% SDS-PAGE and transferred onto nitrocellulose membranes. Membranes were developed with streptavidin conjugated to horse radish peroxidase (HRPO). (B) HT1080 cells were lysed in either 0.8% Brij98/0.2% Triton X-100 or 0.5% CHAPS. Protein complexes were immunoprecipitated with anti-L6-Ag mAb (lane 2), anti-CD151 mAb 5C11 (lane 3), anti-CD81 mAb M38 (lane 4) or anti-CD63 mAb 6H1 (lane 5). Irrelevant mAb (187.1) was used as a negative control (lane 6). The protein lysate (lane 1) was used as a positive control. Immunocomplexes were separated in 11% SDS-PAGE and transferred onto nitrocellulose membranes. Membranes were developed with the mAbs to L6-Ag (L6pke) and with polyclonal anti-CD151 Ab. (C) Co-localisation of L6-Ag with tetraspanins on the surface of BT549 cells. Cells grown on glass coverslips were fixed with 2% paraformaldehyde and subsequently stained with combinations of anti-L6-Ag plus anti-CD63 mAbs (or anti-L6-Ag plus anti-CD9 mAb). Staining was visualised using Alexa-Fluor-594-conjugated goat anti-mouse IgG2a Ab (red) and Alexa-Fluor-488-conjugated goat anti-mouse IgG1 Ab (green). Scale bar: 15 μm.

against tetraspanin CD81 (Fig. 7A, lane 2). These data suggest that L6-Ag might be associated with TERM. Indeed, in further experiments we found that L6-Ag can be co-immunoprecipitated with tetraspanins CD81, CD151 and CD63 (Fig. 7B), and co-localised with them on the surface of BT549 cells (Fig. 7C). Further experiments showed that ~10-15% of the total L6-Ag can be co-immunoprecipitated with various tetraspanins from BT549 and MDA-MB-231 cells (results are not shown). To map the region(s) responsible for the recruitment of L6-Ag to TERM, we analysed the interaction of L6ΔC, L6ΔN and L6Δint mutants with tetraspanins in 293T cells. We also analysed the interaction of L6K[5,86] with tetraspanins. Interestingly, we found that there was a significant reduction in the association of all three deletion/substitution mutants with TERM (Fig. 8A). By contrast, mutation of the ubiquitylation sites had no effect on the interaction (results are not shown). These results indicate that a cytoplasmic linker protein(s) might be required for the effective recruitment of L6-Ag to TERM. It has been shown that the C-terminal cytoplasmic region of L6-Ag interacts with syntenin-2, a PDZ-domain-containing protein (Borrell-Pages et al., 2000). Although syntenin-2 is not expressed in MCF-7 cells (our unpublished results), it was possible that the interaction with another PDZ-domain-containing protein would be important for the recruitment of L6-Ag to TERM and its pro-migratory activity. To address this, we generated a L6CysT mutant in which the C-terminal cysteine[202] was mutated to glycine: it has been reported previously that this mutation would prevent the interaction of L6-Ag with PDZ domains (Borrell-Pages

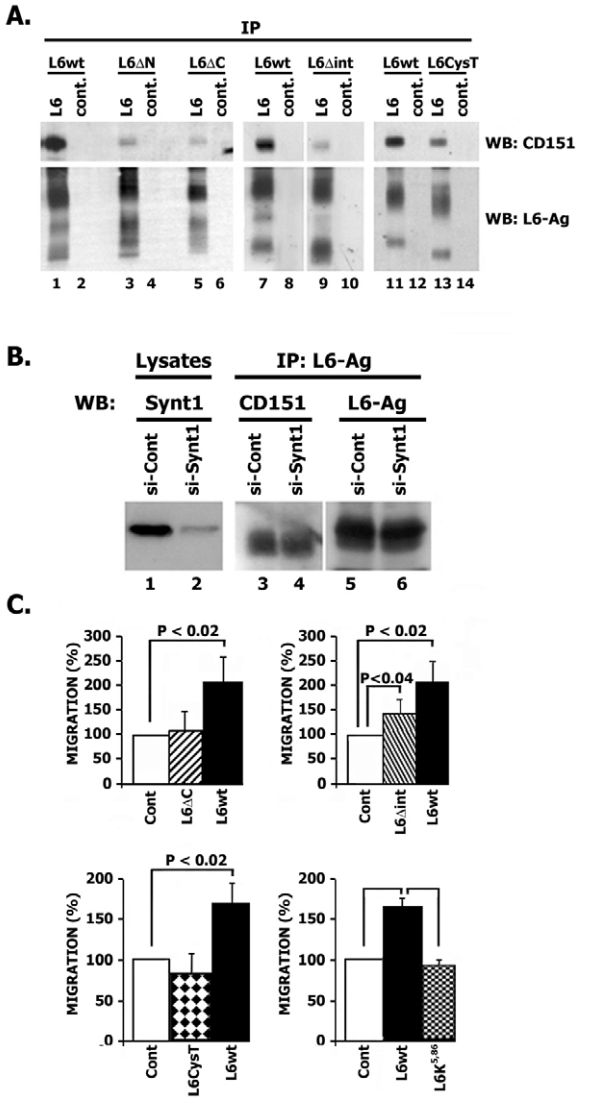

Fig. 8. Association with TERM is essential for the pro-migratory activity of L6-Ag. (A) Predicted cytoplasmic regions are involved in recruitment of L6-Ag to TERM. 293T cells were transiently transfected with the plasmids encoding wild-type L6-Ag or various mutants of L6-Ag. After 48 hours cells were lysed in 0.8% Brij 98/0.2% Triton X-100 and immunoprecipitation was carried out using the anti-L6-Ag mAb (odd lanes) or a negative control mAb (even lanes). Proteins were resolved in 11% SDS-PAGE and transferred to nitrocellulose membranes. The membranes were probed with either anti-CD151 polyclonal Ab or the anti-L6-Ag mAb (L6pke). (B) Syntenin-1 is not involved in the recruitment of L6-Ag to TERM. MDA-MB-231 cells were transiently transfected with either control siRNA (si-Cont) or siRNA that targets syntenin-1 (si-Syn1). After 72 hours cells were lysed in 0.8% Brij 98/0.2% Triton X-100 and immunoprecipitation was carried out using the anti-L6-Ag mAb. Proteins were resolved in 11% SDS-PAGE and transferred to nitrocellulose membranes. The membranes were probed with either anti-CD151 polyclonal Ab or the anti-L6-Ag mAb (L6pke). The degree of syntenin-1 knock-down was assessed by analysing total cell lysates with anti-syntenin-1 mAb (lanes 1 and 2). (C) Effect of L6-Ag mutations on the pro-migratory activity of the protein. MCF-7 cells were co-transfected with plasmids encoding GFP and various L6-Ag constructs. Migration experiments towards fibronectin were performed 48 hours after transfection. Migration was quantified by counting cells in seven random fields per membrane (~10-20 cells/field) as described in detail in Materials and Methods. Data are reported as fold increases over migration of cells transfected with the control plasmid (GFP). Data (all graph panels) are shown as mean ± s.d. calculated from at least three separate experiments each performed in triplicate. *P* values were calculated using the two-tailed *t*-test. L6wt, wild-type L6-Ag.

et al., 2000). Co-immunoprecipitation experiments showed that Cys^{202}→Gly mutation significantly weakened the interaction of L6-Ag with tetraspanins (Fig. 8A, compare lanes 11 and 13). Of note, we observed that the mobility of one of the glycosylated forms of the L6CysT mutant in SDS-PAGE was increased. This suggests that processing of L6-Ag through the Golgi and its glycosylation might be regulated through an interaction involving the C-terminal cysteine. We recently demonstrated that tetraspanin CD63 directly interacts with syntenin-1, a PDZ-domain-containing protein that is closely related to syntenin-2 (Latysheva et al., 2006). Because syntenin-1 has a number of cytoplasmic partners (Sarkar et al., 2004), there was a possibility that it is incorporated in a protein network that would link L6-Ag to TERM. However, we found that depletion of syntenin-1 using specific siRNA did not affect the interaction of L6-Ag with tetraspanins in MDA-MB-231 cells (Fig. 8B).

Association with TERM correlates with the pro-migratory activity of L6-Ag

Because of the established role of tetraspanins in the migration of various cell types, we investigated whether association of L6-Ag with TERM correlates with its pro-migratory activity. Indeed, we found that L6ΔC, L6CysT and L6Δint mutants were deficient in stimulating migration of MCF-7 cells (Fig. 8C). Control experiments showed that the mutations did not affect surface expression of the proteins (results are not shown). The effect of the mutations in the C-terminal region was more pronounced: migration of MCF-7 cells expressing L6ΔC and L6CysT mutants was comparable to that of control cells. By contrast, the L6Δint mutant partially retained its pro-migratory activity. However, even in this case, migration of cells expressing the wild-type protein was significantly higher. Interestingly, although mutations of ubiquitylation sites did not affect recruitment of L6-Ag to TERM, it completely negated the pro-migratory activity of the protein (Fig. 8C). Taken together, these data indicate that, although the association with TERM is necessary for the pro-migratory function of L6-Ag, this is not sufficient and requires ubiquitylation of the protein.

L6-Ag regulates surface expression of tetraspanins

Induced overexpression or downregulation of various tetraspanins in various cell types changes their migratory potential (Hemler, 2005). We therefore examined whether L6-Ag influences migration of breast cancer cells by regulating expression levels of tetraspanins. Flow cytometry experiments showed that downregulation of L6-Ag in BT549 cells resulted in significant increases in surface levels of tetraspanin CD63 (~2.5-fold) and CD82 (~40%) (Fig. 9A). Conversely, overexpression of the wild-type L6-Ag (but not $L6K^{5,86}$) in MCF-7 cells decreased the expression levels of CD63 (Fig. 9B). By contrast, the surface levels of two other tetraspanins (CD81 and CD151) and integrins α3β1 and α6β1 were comparable in BT549/$L6^{high}$ and BT549/$L6^{low}$ cells. Importantly, downregulation of L6-Ag did not change total levels of tetraspanins in BT549 cells (Fig. 9C). We also observed that downregulation of L6-Ag affected intracellular distribution of CD63: in ~50-60% of BT549/$L6^{low}$ cells, CD63-positive vesicles were more evenly scattered through the cytoplasm than they were in control cells (Fig. 9D). By contrast, <10% of BT549/$L6^{high}$ cells display this phenotype. Whilst doing this analysis we noticed that L6-Ag-negative BT549 cells spread slightly better than cells expressing high levels of the protein (spreading area of BT549/$L6^{low}$ cells was ~20-40% larger than that of BT549/$L6^{high}$ cells). Thus, it is possible that differences in cell

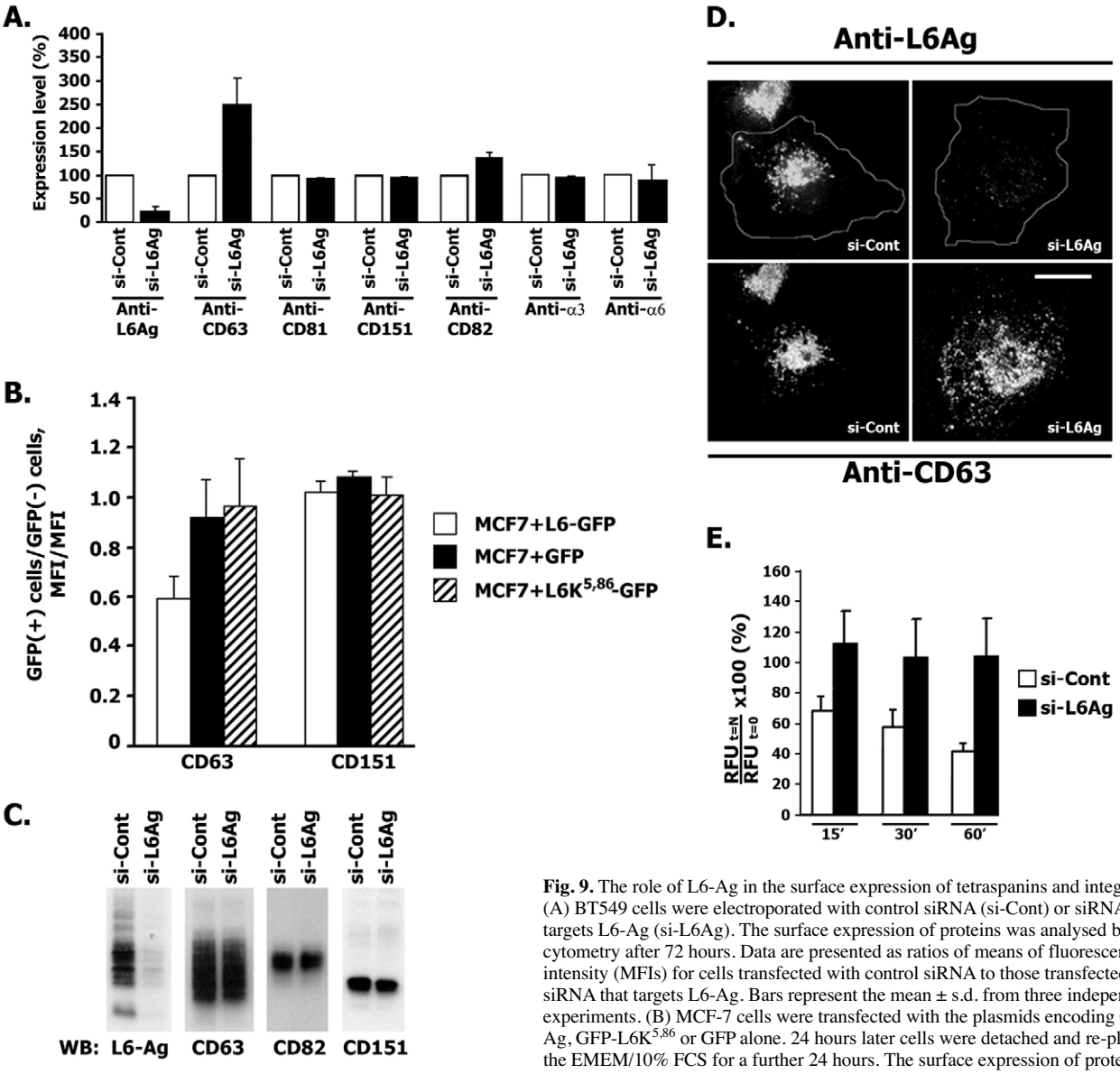

Fig. 9. The role of L6-Ag in the surface expression of tetraspanins and integrins. (A) BT549 cells were electroporated with control siRNA (si-Cont) or siRNA that targets L6-Ag (si-L6Ag). The surface expression of proteins was analysed by flow cytometry after 72 hours. Data are presented as ratios of means of fluorescence intensity (MFIs) for cells transfected with control siRNA to those transfected with siRNA that targets L6-Ag. Bars represent the mean ± s.d. from three independent experiments. (B) MCF-7 cells were transfected with the plasmids encoding GFP-L6-Ag, GFP-L6K^{5,86} or GFP alone. 24 hours later cells were detached and re-plated in the EMEM/10% FCS for a further 24 hours. The surface expression of proteins was analysed by flow cytometry. Data presented as ratios of means of fluorescence intensity (MFIs) for cells expressing GFP-proteins to those of non-transfected cells. Bar values represent the mean ± s.d. from three independent experiments. (C) Lysates prepared from cells transfected with control siRNA and siRNA that targets L6Ag (as described in A) were resolved in 11% SDS-PAGE and transferred to nitrocellulose membranes. The membranes were probed with anti-CD151 polyclonal Ab, the anti-L6-Ag mAb (L6pke), anti-CD82 mAb (TS82) and anti-CD63 mAb (1C5). Shown are the results of a representative experiment. (D) BT549 cells were electroporated with control siRNA or siRNA that targets L6-Ag. Intracellular distribution of proteins after 72 hours was analysed as described in Fig. 2. Note that CD63-positive vesicles are more evenly scattered through the cytoplasm in cells in which the expression of L6-Ag was knocked down by siRNA than controls. (E) BT549 cells were electroporated with control siRNA or siRNA that targets L6-Ag. 72 hours later cells were surface labelled with the anti-CD63 mAb 6H1 for 1 hour at 4°C and then placed to 37°C for the indicated durations. Non-internalised mAbs were labelled with IRDye-800CW-conjugated goat anti-mouse IgG. Fluorescent signals were detected using Odyssey infrared imaging system. Data is presented as percentage of the mAb 6H1 left on the cell surface relative to that at time point 0, t=0 (100%, fluorescent signals before cell were placed to 37°C) and are shown as mean ± s.d. calculated from at least three separate experiments each performed in triplicate. RFU t=N, relative fluorescence units at a given time interval; RFU t=0, relative fluorescence units at time point 0. Scale bar: 10 μm.

spreading can account for the changes in the distribution of CD63-positive organelles. Alternatively, altered trafficking/dynamics of these vesicles might affect cell spreading. Finally, we analysed the effect of L6-Ag depletion on endocytosis of CD63. In BT549 cells transfected with control siRNA, we observed progressive clearance of the surface-bound anti-CD63 mAb over 1 hour (Fig. 9E). By contrast, the level of CD63 on the surface of BT549/L6^{low} cells remained practically unchanged over this period of time. These results strongly suggest that L6-Ag affects various aspects of CD63 trafficking.

Discussion

In this article we show that L6-Ag is a novel component of TERM and that this association is crucial for the pro-migratory activity of the protein. We also found that L6-Ag regulates surface expression of at least two tetraspanin proteins, CD63 and CD82. This suggests

that the pro-migratory activity of the protein is linked to the reorganisation within TERM.

A number of overexpression and downregulation experiments have shown that the expression levels of both CD63 and CD82 inversely correlate with motility of various cell types (Jee et al., 2007; Mantegazza et al., 2004; Radford et al., 1997; Yang et al., 2001; Zhang et al., 2003). Although in most of these studies the underlying molecular mechanisms were not examined, it was proposed that modulation in the expression levels of tetraspanins could affect signalling via the transmembrane receptors associated with TERM (e.g. integrins, receptor tyrosine kinases). Indeed, overexpression of CD82 in prostate cancer cells resulted in alterations in the FAK-Lyn-p130CAS-CrkII signalling pathway, which correlated with decreased cell motility (Zhang et al., 2003). CD82 is also known to regulate signalling via EGFR and c-Met (Odintsova et al., 2000; Sridhar and Miranti, 2006). In addition, recent data suggest that both CD82 and CD63 might be involved in the regulation of surface expression of integrins (He et al., 2005; Jee et al., 2007; Mantegazza et al., 2004). However, our results showed that there were no corresponding changes in the expression levels of CD63 and CD82 and TERM-associated β1 integrins on the surface of BT549/L6^{high} and BT549/L6^{low} cells. Furthermore, we found no evidence linking L6-Ag to the FAK-p130Cas signalling pathway (results are not shown). This suggests that, if CD63 and CD82 are indeed the key players in L6-Ag-dependent migration, they are likely to target alternative signalling pathways. It is feasible that these involve L6-Ag-associated cytoplasmic proteins that either link L6-Ag to TERM (see below) or/and are recruited to an ubiquitylated form of L6-Ag. Ubiquitylation of L6-Ag, in turn, might prove to be an important factor in regulating the dynamics of CD63 on the plasma membrane. Indeed, ubiquitylation of various transmembrane proteins is known to provide a scaffolding platform for the recruitment of cytoplasmic proteins involved in endocytic trafficking (Mukhopadhyay and Riezman, 2007). Although ubiquitylation is not required for targeting of L6-Ag to late endocytic organelles (also see below), L6-Ag-dependent juxtaposition of the endocytic scaffold to TERM might influence the dynamics of the associated proteins on the plasma membrane.

L6-Ag represents an example of a transmembrane protein that is linked to TERM via its cytoplasmic regions. Similarly, an earlier study showed that the cytoplasmic domain of CD4 is required for its association with CD81 and CD82 (Imai et al., 1995). Importantly, efficient recruitment of L6-Ag to TERM seems to require all three predicted cytoplasmic domains of the protein. Thus, one possibility is that the link is provided by a protein that makes multiple contacts with L6-Ag. The only known cytoplasmic partner of L6-Ag is syntenin-2, a PDZ-domain-containing protein that might be involved in cell proliferation and survival (Mortier et al., 2005). Although we found that mutation of the crucial cysteine in the C-terminal cytoplasmic region of L6-Ag has a clear negative effect on its association with TERM (and abolishes the pro-migratory activity of the protein), the fact that both MCF-7 and MDA-MB-231 cells express negligible amounts of endogenous syntenin-2 makes it an unlikely candidate for providing a physical link between L6-Ag and tetraspanins. We also found that L6-Ag does not interact with three other PDZ-domain-containing proteins that are known to bind peptide ligands that end with cysteine [i.e. synectin (GIPC, TIP-2) (Ligensa et al., 2001), PTP-H1 (Zheng et al., 2002) and PTP-BL (Gross et al., 2001)] (results are not shown). Alternatively, various mutations that we introduced into cytoplasmic regions of L6-Ag might potentially influence post-translation modifications of the protein (e.g. glycosylation, palmitoylation) and thereby affect its recruitment to TERM. In this regard, we and others have previously shown that palmitoylation could influence heterotypic protein interactions within TERM (Berditchevski et al., 2002; Charrin et al., 2002; Yang et al., 2002). Finally, mutations in the cytoplasmic regions might have altered the overall conformation of L6-Ag and, thus, its ability to associate with tetraspanin proteins. Although we cannot completely rule out this possibility, the fact that binding of two anti-L6 mAbs and subcellular distribution of the protein at the level of fluorescence microscopy was not affected argues against this interpretation of our data.

Not only will the identification of the linker protein clarify structural and signalling aspects of the L6-Ag–TERM connection and support a new paradigm of heterotypic interactions between transmembrane proteins within TERM, it might also provide a mechanistic insight into how L6-Ag regulates surface expression of CD63 and CD82. Trafficking of CD63 is regulated by adaptor protein complexes AP2 and AP3, which bind to the tyrosine-based sorting motif in the C-terminal cytoplasmic domain of the tetraspanin (Janvier and Bonifacino, 2005; Rous et al., 2002). The same region of CD63 also interacts with syntenin-1, which might, therefore, function as a competitive inhibitor for AP2/AP3 binding and, thus, divert trafficking of the tetraspanin from the 'classical', AP-dependent pathways (Latysheva et al., 2006). Although thus far we found no evidence supporting the direct role of syntenin-1 in L6-Ag-mediated stabilisation of CD63 on the plasma membrane, it is feasible that the concept of 'shielding' (or competitive inhibition of AP2/AP3 binding) by a putative L6-Ag-associated cytoplasmic partner explains the effect of L6-Ag on trafficking of tetraspanins.

Subcellular distribution of L6-Ag almost completely overlaps with that of CD63. Nonetheless, at least one aspect of their trafficking to LEO is clearly distinct. Although CD63 is readily targeted to LEO from the cell surface (Mantegazza et al., 2004; Rous et al., 2002), our results strongly suggest that a biosynthetic pathway is the main route of delivery of L6-Ag to late endosomes. First, we established that there is no persistent centripetal trafficking of L6-Ag towards centrally located LEO. Second, there was no apparent internalisation of the surface-bound anti-L6-Ag mAb over the whole period of observation (7-24 hours). Although these data do not exclude a possibility that a small proportion of the protein can be targeted to LEO from the plasma membrane, they are indicative of a minimal contribution of the constitutive endocytosis in the targeting process. Because L6-Ag does not possess any of the known targeting/sorting motifs, it is likely that its trafficking towards late endosomes requires the activity(ies) of the associated protein(s). The fact that the presence of transmembrane domains is sufficient for trafficking L6-Ag to LEO suggests that at least one additional transmembrane protein is involved in the targeting process. In this regard, the contribution of a transmembrane region in targeting to LEO has been previously observed for LGP85, a member of the CD36 superfamily (Kuronita et al., 2005). Although it was previously reported that syntenin-2 affects the subcellular localisation of L6-Ag (Borrell-Pages et al., 2000), our results clearly indicate that this or any other possible interactions involving the C-terminal cysteine are not essential for the localisation of L6-Ag to late endocytic compartments in MCF-7 cells. Surprisingly, although L6-Ag is ubiquitylated (molecular masses of ubiquitylated species of L6-Ag suggest that the protein undergoes mono- and di-ubiquitylation), mutations of ubiquitylation sites does not preclude trafficking of the protein to

LEO. Nevertheless, subtle differences observed in the distribution of wild-type L6-Ag and its ubiquitylation-deficient mutant suggest that, in addition to its role in cell motility at the plasma membrane, ubiquitylation of the protein might be important for intracellular function of the protein.

In summary, we have identified a new mode of regulation within TERM in which one of its transmembrane components controls the dynamics of the others. Our data also point to a previously unknown link between cell motility and ubiquitylation of proteins within TERM. L6-Ag-dependent recruitment of cytoplasmic proteins to TERM might be directly responsible for both destabilising TERM on the plasma membrane of and providing downstream targets for certain tetraspanins in migrating cancer cells.

Materials and Methods

Cell lines and antibodies

MCF-7, Cos-7, 293T, HT1080, MDA-MB-231 and HeLa cells were grown in DMEM (Sigma) supplemented with 10% FCS. BT549 cells were grown in RPMI-1640 media supplemented with 10% FCS. The mouse anti-CD81 and anti-CD82 mAbs (M38 and M104, respectively) were kindly provided by O. Yoshie (Kinki University School of Medicine, Osaka, Japan). The anti-CD63 (6H1) and anti-CD151 (5C11) mAbs were described previously (Berditchevski et al., 1997; Berditchevski et al., 1995). The anti-CD9 (Syb1) and anti-CD82 (TS82) mAbs were generously provided by E. Rubinstein (INSERM U602, Villejuif, France). The anti-integrin mAbs used were A2-VIIC6, anti-α2 (Berditchevski and Odintsova, 1999); A3-IVA5, anti-α3 (Weitzman et al., 1993); P1D6, anti-α5 (Wayner and Carter, 1987); and A6-ELE, anti-α6 (Tachibana et al., 1997). The mAb anti-Golgi 58K protein (clone 58K-9) was purchased from Sigma. The mouse anti-EEA1 mAbs were purchased from BD Biosciences. The mouse anti-CD63 mAb (1C5) were provided by M. Marsh (UCL, London, UK). The anti-LBPA mAb (6C4) was provided by J. Gruenberg (University of Geneva, Geneva). The mouse mAbs to human Lamp1 and Lamp2 were from the Development Studies Hybridoma Bank. The anti-rabbit polyclonal Abs to CD151 were provided by L. Ashman (University of Newcastle, Newcastle, Australia). The mouse mAbs to L6-Ag were from S. Roffler (Institute of Biomedical Sciences, Taipei, Taiwan) and B. Schäfer (Universität des Saarlandes, Homburg, Germany). The monoclonal and polyclonal anti-HA-tag Abs (F7 and Y-11, respectively) were purchased from Autogen Bioclear.

Plasmids and transfection

The cDNA encoding human L6-Ag was subcloned from pPS1170C pxLNC-L6ag (provided by P. Searle, University of Birmingham, UK) into pcDNA3neo and pZeoSV. Plasmid encoding the HA-tagged form of human ubiquitin was provided by A. Turnell (University of Birmingham, UK). Transfection experiments were carried out using Fugene 6 (Roche) according to the manufacturer's instructions. For transfection with siRNA, cells were transfected with 1 μg of pre-annealed siRNA using either siPORT NeoFX (Ambion) according to the manufacturer's protocol or electroporation. The following siRNAs were found to be effective in knock-down experiments: L6-Ag, 5′-CCACUAUGUCUUGAUUCCCtt-3′; 5′-GGGCACACUUUCAUCUAAUtt-3′. *Silencer* negative control #1 siRNA was purchased from Ambion (catalogue # 4611).

Immunoprecipitation and western blotting

The proteins were solubilised into the immunoprecipitation buffer containing 0.5% CHAPS/PBS (or 0.8% Brij98/0.2% Triton X-100/PBS), 2 mM phenylmethylsulfonyl fluoride, 10 μg/ml aprotinin, 10 μg/ml leupeptin for 2 hours at 4°C. The insoluble material was pelleted at 12,000 ***g*** for 10 minutes. The cell lysates were then precleared by incubation for 2 hours at 4°C with agarose beads conjugated with goat anti-mouse antibodies (mIgG-beads, Sigma). Immune complexes were collected using appropriate mAbs prebound to the mIgG beads and washed four times with the immunoprecipitation buffer. The complexes were eluted from the beads with Laemmli sample buffer. Proteins were resolved in SDS-PAGE, transferred to the nitrocellulose membrane and developed with the appropriate Ab. Protein bands were visualised using horseradish peroxidase-conjugated secondary antibodies (Sigma) and enhanced chemiluminescence reagent (Amersham Pharmacia Biochem).

Immunofluorescence staining

Cells were grown on glass coverslips in complete media for 24-72 hours. Spread cells were fixed with 2% paraformaldehyde/PBS for 10-15 minutes. The staining with primary and fluorochrome-conjugated secondary Abs was carried out as previously described (Berditchevski and Odintsova, 1999). The staining was analysed using the Nikon Eclipse E600 microscope. Images were acquired using the Leica DC200 digital camera and subsequently processed using the DC200 image-processing programme. Confocal images were acquired using a LSM510 microscope and Carl Zeiss LSM Image software (Carl Zeiss Laser Scanning System) with 60× oil-immersion objective (NA 0.8 mm).

Antibody uptake/pulse-chase

Cells were incubated with 10 μg/ml L6 IgG_{2a} or mAb 6H1 for 1 hour at 4°C. Cells were rinsed three times with ice-cold PBS (zero time point, T0) and then transferred to pre-warmed complete growth media at 37°C for different lengths of time (10 minutes, 1, 4, 7 and 24 hours). At each time point, a set of coverslips was taken out the incubator and cells were immediately fixed for 20 minutes with 2% PFA at room temperature. The fixed cells were kept in PBS at 4°C until the completion of the experiment. At the end of the last time point, all cells were permeabilised for 2 minutes in 0.1% Triton X-100. Cells were then rinsed in PBS and blocked for 1 hour with blocking buffer (20% heat-inactivated normal goat serum/PBS). After blocking, cells were incubated with FITC-conjugated goat anti-mouse Ab (1:100 in blocking buffer) for 1 hour at room temperature. Finally, cells were rinsed in PBS and water. Coverslips were subsequently processed for analysis as described above. For quantification of anti-CD63 mAb uptake, BT549 cells were transfected with the appropriate siRNA and labelled with the mAb at 4°C as above. Internalisation of the surface-bound mAb was analysed using Odyssey infrared imaging system (LI-COR Biosciences) according to the manufacturer's protocol.

Migration assay

Migration was analysed using a standard Boyden Chamber protocol. In brief, 2.5×10^5 to 3×10^5 cells suspended in 100-150 μl serum-free DMEM were aliquoted into the inner compartment of Nunc's tissue culture inserts 8-μM pore size polycarbonate membranes, the bottom sides of which were coated with 10 μg/ml fibronectin. Cells were allowed to migrate towards complete media for 3-24 hours. Non-migrated cells were removed and nuclei of migrating cells were stained with DAPI. Membranes were mounted on glass slides and analysed using a Nikon Eclipse E600 microscope. Seven random fields per membrane were counted under microscope or pictures were taken and analysed using ImageJ nuclear/cell counter programme. Each of the experiments was done in triplicate and at least three independent experiments were carried out for each cell line.

Flow cytometry

Cells were incubated with saturating concentrations of primary mouse mAbs for 45 minutes at 4°C, washed twice and then labelled with phycoeritrin (PE)-conjugated goat anti-mouse immunoglobulin. Stained cells were analysed on a FACScan (Becton Dickinson, UK).

We are very grateful to all our colleagues for their generous gifts of the reagents that were used in this study. This work was supported by CR UK studentship grant C1322 (to E.F. and F.B.) and Breast Cancer Campaign grant 2003:574 (to M.M., T.L. and F.B.).

References

Berditchevski, F. (2001). Complexes of tetraspanins with integrins:more than meets the eye. *J. Cell Sci.* **115**, 4143-4151.

Berditchevski, F. and Odintsova, E. (1999). Characterization of integrin/tetraspanin adhesion complexes: role of tetraspanins in integrin signaling. *J. Cell Biol.* **146**, 477-492.

Berditchevski, F., Bazzoni, G. and Hemler, M. E. (1995). Specific association of CD63 with the VLA-3 and VLA-6 integrins. *J. Biol. Chem.* **270**, 17784-17790.

Berditchevski, F., Chang, S., Bodorova, J. and Hemler, M. E. (1997). Generation of monoclonal antibodies to integrin-associated proteins. Evidence that alpha3beta1 complexes with EMMPRIN/basigin/OX47/M6. *J. Biol. Chem.* **272**, 29174-29180.

Berditchevski, F., Odintsova, E., Sawada, S. and Gilbert, E. (2002). Expression of the palmitoylation-deficient CD151 weakens the association of alpha 3 beta 1 integrin with the tetraspanin-enriched microdomains and affects integrin-dependent signaling. *J. Biol. Chem.* **277**, 36991-37000.

Bonifacino, J. S. and Traub, L. M. (2003). Signals for sorting of transmembrane proteins to endosomes and lysosomes. *Annu. Rev. Biochem.* **72**, 395-447.

Borrell-Pages, M., Fernandez-Larrea, J., Borroto, A., Rojo, F., Baselga, J. and Arribas, J. (2000). The carboxy-terminal cysteine of the tetraspanin L6 antigen is required for its interaction with SITAC, a novel PDZ protein. *Mol. Biol. Cell* **11**, 4217-4225.

Chang, Y. W., Chen, S. C., Cheng, E. C., Ko, Y. P., Lin, Y. C., Kao, Y. R., Tsay, Y. G., Yang, P. C., Wu, C. W. and Roffler, S. R. (2005). CD13 (aminopeptidase N) can associate with tumor-associated antigen L6 and enhance the motility of human lung cancer cells. *Int. J. Cancer* **116**, 243-252.

Charrin, S., Manié, S., Qualid, M., Billard, M., Boucheix, C. and Rubinstein, E. (2002). Differential stability of tetraspanin/tetraspanin interactions: role of palmitoylation. *FEBS Lett.* **516**, 139-144.

Edwards, C. P., Farr, A. G., Marken, J. S., Nelson, A., Bajorath, J., Hellstrom, K. E., Hellstrom, I. and Aruffo, A. (1995). Cloning of the murine counterpart of the tumor-associated antigen H-L6: epitope mapping of the human and murine L6 antigens. *Biochemistry* **34**, 12653-12660.

Fabbri, M., Di M. S., Gagliani, M. C., Consonni, E., Molteni, R., Bender, J. R., Tacchetti, C. and Pardi, R. (2005). Dynamic partitioning into lipid rafts controls the endo-exocytic cycle of the alphaL/beta2 integrin, LFA-1, during leukocyte chemotaxis. *Mol. Biol. Cell* **16**, 5793-5803.

Gross, C., Heumann, R. and Erdmann, K. S. (2001). The protein kinase C-related kinase PRK2 interacts with the protein tyrosine phosphatase PTP-BL via a novel PDZ domain binding motif. *FEBS Lett.* **496**, 101-104.

He, B., Liu, L., Cook, G. A., Grgurevich, S., Jennings, L. K. and Zhang, X. A. (2005). Tetraspanin CD82 attenuates cellular morphogenesis through down-regulating integrin alpha6-mediated cell adhesion. *J. Biol. Chem.* **280**, 3346-3354.

Hellström, I., Horn, D., Linsley, P., Brown, J. P., Brankovan, V. and Hellström, K. E. (1986). Monoclonal mouse antibodies raised against human lung cancer. *Cancer Res.* **46**, 3917-3923.

Hemler, M. E. (2005). Tetraspanin functions and associated microdomains. *Nat. Rev. Mol. Cell Biol.* **6**, 801-811.

Imai, T., Kakizaki, M., Nishimura, M. and Yoshie, O. (1995). Molecular analysis of the association of CD4 with two members of the transmembrane 4 superfamily, CD81 and CD82. *J. Immunol.* **155**, 1229-1239.

Ivaska, J., Whelan, R. D., Watson, R. and Parker, P. J. (2002). PKC epsilon controls the traffic of beta1 integrins in motile cells. *EMBO J.* **21**, 3608-3619.

Janvier, K. and Bonifacino, J. S. (2005). Role of the endocytic machinery in the sorting of lysosome-associated membrane proteins. *Mol. Biol. Cell* **16**, 4231-4242.

Jee, B. K., Lee, J. Y., Lim, Y., Lee, K. H. and Jo, Y. H. (2007). Effect of KAI1/CD82 on the beta1 integrin maturation in highly migratory carcinoma cells. *Biochem. Biophys. Res. Commun.* **359**, 703-708.

Jones, M. C., Caswell, P. T. and Norman, J. C. (2006). Endocytic recycling pathways: emerging regulators of cell migration. *Curr. Opin. Cell Biol.* **18**, 549-557.

Kao, Y. R., Shih, J. Y., Wen, W. C., Ko, Y. P., Chen, B. M., Chan, Y. L., Chu, Y. W., Yang, P. C., Wu, C. W. and Roffler, S. R. (2003). Tumor-associated antigen L6 and the invasion of human lung cancer cells. *Clin. Cancer Res.* **9**, 2807-2816.

Koroll, M., Rathjen, F. G. and Volkmer, H. (2001). The neural cell recognition molecule neurofascin interacts with syntenin-1 but not with syntenin-2, both of which reveal self-associating activity. *J. Biol. Chem.* **276**, 10646-10654.

Kuronita, T., Hatano, T., Furuyama, A., Hirota, Y., Masuyama, N., Saftig, P., Himeno, M., Fujita, H. and Tanaka, Y. (2005). The NH(2)-terminal transmembrane and lumenal domains of LGP85 are needed for the formation of enlarged endosomes/lysosomes. *Traffic* **6**, 895-906.

Latysheva, N., Muratov, G., Rajesh, S., Padgett, M., Hotchin, N. A., Overduin, M. and Berditchevski, F. (2006). Syntenin-1 is a new component of tetraspanin-enriched microdomains: mechanisms and consequences of the interaction of syntenin-1 with CD63. *Mol. Cell. Biol.* **26**, 7707-7718.

Leube, R. E. (1995). The topogenic fate of the polytopic transmembrane proteins, synaptophysin and connexin, is determined by their membrane-spanning domains. *J. Cell Sci.* **108**, 883-894.

Li, J., Ballif, B. A., Powelka, A. M., Dai, J., Gygi, S. P. and Hsu, V. W. (2005). Phosphorylation of ACAP1 by Akt regulates the stimulation-dependent recycling of integrin beta1 to control cell migration. *Dev. Cell* **9**, 663-673.

Ligensa, T., Krauss, S., Demuth, D., Schumacher, R., Camonis, J., Jaques, G. and Weidner, K. M. (2001). A PDZ domain protein interacts with the C-terminal tail of the insulin-like growth factor-1 receptor but not with the insulin receptor. *J. Biol. Chem.* **276**, 33419-33427.

Mantegazza, A. R., Barrio, M. M., Moutel, S., Bover, L., Weck, M., Brossart, P., Teillaud, J. L. and Mordoh, J. (2004). CD63 tetraspanin slows down cell migration and translocates to the endosomal-lysosomal-MIICs route after extracellular stimuli in human immature dendritic cells. *Blood* **104**, 1183-1190.

Marken, J. S., Schieven, G. L., Hellstrom, I., Hellstrom, E. and Aruffo, A. (1992). Cloning and expression of the tumor-associated antigen L6. *Proc. Natl. Acad. Sci. USA* **89**, 3503-3507.

Mortier, E., Wuytens, G., Leenaerts, I., Hannes, F., Heung, M. Y., Degeest, G., David, G. and Zimmermann, P. (2005). Nuclear speckles and nucleoli targeting by PIP2-PDZ domain interactions. *EMBO J.* **24**, 2556-2565.

Mukhopadhyay, D. and Riezman, H. (2007). Proteasome-independent functions of ubiquitin in endocytosis and signaling. *Science* **315**, 201-205.

Muller-Pillasch, F., Wallrapp, C., Lacher, U., Friess, H., Buchler, M., Adler, G. and Gress, T. M. (1998). Identification of a new tumour-associated antigen TM4SF5 and its expression in human cancer. *Gene* **208**, 25-30.

Odintsova, E., Sugiura, T. and Berditchevski, F. (2000). Attenuation of EGF receptor signaling by a metastasis suppressor tetraspanin KAI-1/CD82. *Curr. Biol.* **10**, 1009-1012.

Radford, K. J., Thorne, R. F. and Hersey, P. (1997). Regulation of tumor cell motility and migration by CD63 in a human melanoma cell line. *J. Immunol.* **158**, 3353-3358.

Raiborg, C., Rusten, T. E. and Stenmark, H. (2003). Protein sorting into multivesicular endosomes. *Curr. Opin. Cell Biol.* **15**, 446-455.

Roberts, M., Barry, S., Woods, A., van der Sluijs, P. and Norman, J. (2001). PDGF-regulated rab4-dependent recycling of alphavbeta3 integrin from early endosomes is necessary for cell adhesion and spreading. *Curr. Biol.* **11**, 1392-1402.

Rous, B. A., Reaves, B. J., Ihrke, G., Briggs, J. A., Gray, S. R., Stephens, D. J., Banting, G. and Luzio, J. P. (2002). Role of adaptor complex AP-3 in targeting wild-type and mutated CD63 to lysosomes. *Mol. Biol. Cell* **13**, 1071-1082.

Sarkar, D., Boukerche, H., Su, Z. Z. and Fisher, P. B. (2004). mda-9/syntenin: recent insights into a novel cell signaling and metastasis-associated gene. *Pharmacol. Ther.* **104**, 101-115.

Sawada, S., Yoshimoto, M., Odintsova, E., Hotchin, N. A. and Berditchevski, F. (2003). The tetraspanin CD151 functions as a negative regulator in the adhesion-dependent activation of Ras. *J. Biol. Chem.* **278**, 26323-26326.

Shigeta, M., Sanzen, N., Ozawa, M., Gu, J., Hasegawa, H. and Sekiguchi, K. (2003). CD151 regulates epithelial cell-cell adhesion through PKC- and Cdc42-dependent actin cytoskeletal reorganization. *J. Cell Biol.* **163**, 165-176.

Shoham, T., Rajapaksa, R., Boucheix, C., Rubinstein, E., Poe, J. C., Tedder, T. F. and Levy, S. (2003). The tetraspanin CD81 regulates the expression of CD19 during B cell development in a postendoplasmic reticulum compartment. *J. Immunol.* **171**, 4062-4072.

Sridhar, S. C. and Miranti, C. K. (2006). Tetraspanin KAI1/CD82 suppresses invasion by inhibiting integrin-dependent crosstalk with c-Met receptor and Src kinases. *Oncogene* **25**, 2367-2378.

Storim, J., Friedl, P., Schaefer, B. M., Bechtel, M., Wallich, R., Kramer, M. D. and Reinartz, J. (2001). Molecular and functional characterization of the four-transmembrane molecule l6 in epidermal keratinocytes. *Exp. Cell Res.* **267**, 233-242.

Sugiura, T. and Berditchevski, F. (1999). Function of α3β1-tetraspanin protein complexes in tumor cell invasion. Evidence for the role of the complexes in production of Matrix Metalloproteinase 2 (MMP-2). *J. Cell Biol.* **146**, 1375-1389.

Tachibana, I., Bodorova, J., Berditchevski, F., Zutter, M. M. and Hemler, M. E. (1997). NAG-2, a novel transmembrane-4 superfamily (TM4SF) protein that complexes with integrins and other TM4SF proteins. *J. Biol. Chem.* **272**, 29181-29189.

Takeda, Y., Kazarov, A. R., Butterfield, C. E., Hopkins, B. D., Benjamin, L. E., Kaipainen, A. and Hemler, M. E. (2007). Deletion of tetraspanin CD151 results in decreased pathological angiogenesis in vivo and in vitro. *Blood* **109**, 1524-1532.

Wayner, E. A. and Carter, W. G. (1987). Identification of multiple cell adhesion receptors for collagen and fibronectin in human fibrosarcoma cells possessing unique alpha and common beta subunits. *J. Cell Biol.* **105**, 1873-1884.

Weitzman, J. B., Pasqualini, R., Takada, Y. and Hemler, M. E. (1993). The function and distinctive regulation of the integrin VLA-3 in cell adhesion, spreading and homotypic cell aggregation. *J. Biol. Chem.* **268**, 8651-8657.

White, D. P., Caswell, P. T. and Norman, J. C. (2007). alpha v beta3 and alpha5beta1 integrin recycling pathways dictate downstream Rho kinase signaling to regulate persistent cell migration. *J. Cell Biol.* **177**, 515-525.

Wice, B. M. and Gordon, J. I. (1995). A tetraspan membrane glycoprotein produced in the human intestinal epitheliul and liver that can regulate cell density-dependent proliferation. *J. Biol. Chem.* **270**, 21907-21918.

Winterwood, N. E., Varzavand, A., Meland, M. N., Ashman, L. K. and Stipp, C. S. (2006). A critical role for tetraspanin CD151 in alpha3beta1 and alpha6beta4 integrin-dependent tumor cell functions on laminin-5. *Mol. Biol. Cell* **17**, 2707-2721.

Wright, M. D. and Tomlinson, M. G. (1994). The ins and outs of the transmembrane 4 superfamily. *Immunol. Today* **15**, 588-594.

Wright, M. D., Ni, J. and Rudy, G. B. (2000). The L6 membrane proteins-a new four-transmembrane superfamily. *Protein Sci.* **9**, 1594-1600.

Yang, X., Wei, L. L., Tang, C., Slack, R. and Lippman, M. E. (2001). Overexpression of KAI1 suppresses in vitro invasiveness and in vivo metastasis in breast cancer cells. *Cancer Res.* **61**, 5284-5288.

Yang, X., Claas, C., Kraeft, S.-K., Chen, L. B., Wang, Z., Kriedberg, J. A. and Hemler, M. E. (2002). Palmitoylation of tetraspanin proteins: modulation of CD151 lateral interactions, subcellular distribution, and integrin-dependent cell morphology. *Mol. Biol. Cell* **13**, 767-781.

Zhang, X. A., He, B., Zhou, B. and Liu, L. (2003). Requirement of the p130CAS-Crk coupling for metastasis suppressor KAI1/CD82-mediated inhibition of cell migration. *J. Biol. Chem.* **278**, 27319-27328.

Zheng, Y., Schlondorff, J. and Blobel, C. P. (2002). Evidence for regulation of the tumor necrosis factor alpha-convertase (TACE) by protein-tyrosine phosphatase PTPH1. *J. Biol. Chem.* **277**, 42463-42470.